Proceedings of the 12th International Conference on Fluid Flow, Heat and Mass Transfer (FFHMT 2025)
July 15, 2025 - July 17, 2025 | Imperial College London Conference, London, United Kingdom
Paper No. 125
DOI: 10.11159/ffhmt25.125

Experimental Investigation of Two-Phase Flows in Microchannels & Onset of Flooding For NH_3/H_2O Absorption Systems Using Simulating Fluids

SLEIMAN Jana[1,2], STUTZ Benoit[2], CHANDEZ Bertrand[1], PHAN Hai Trieu[1]
[1]Université Grenoble Alpes, CEA, LITEN, Campus INES
73375 Le Bourget du Lac, France
Jana.sleiman@cea.fr; haitrieu.phan@cea.fr; bertrand.chandez@cea.fr
[2]Université Savoie Mont Blanc, CNRS, LOCIE
73376 Le Bourget du Lac, France
Benoit.stutz@univ-smb.fr

Abstract **-** The rising demand for cooling, driven by increasing summertime temperatures, has traditionally been met by mechanical compression air conditioners, which rely on high electricity consumption. Absorption chillers offer a sustainable alternative, leveraging renewable heat sources such as solar energy or industrial waste heat. However, the large size and high initial costs of their components remain significant barriers to their widespread adoption. This study contributes to the development of compact and cost-effective NH_3/H_2O absorption chillers utilizing plate heat exchangers. An experimental setup was designed to examine the hydrodynamic behavior of liquid-vapor two-phase flows within vertical plate heat exchangers under varying confinement levels. The counter-current flow configuration, representative of conditions within the generator of an absorption chiller, was chosen due to its susceptibility to the flooding phenomena that should be avoided to ensure reliable operation of the system. The research focuses on identifying the conditions leading to the onset of flooding as well as the falling film patterns within these plate heat exchangers using air-water as simulating fluids, providing useful insights to enhance the performance and compactness of absorption chillers.

Keywords**:** Counter-current – two-phase flow – Onset of flooding – Microchannels – Falling film

1. Introduction

The growing refrigeration demand [1] , driven by rising temperatures and increasing urbanization has intensified the need for sustainable solutions. Absorption chillers have emerged as an encouraging alternative to conventional air-conditioning systems by utilizing heat as their primary energy source. These systems frequently rely on sustainable energy options, such as solar radiation or industrial waste heat. By mitigating dependence on electrical grids, absorption chillers significantly contribute also to lowering greenhouse gas emissions and addressing environmental challenges. Additionally, they operate with natural refrigerants, which have lower environmental impact compared to the synthetic refrigerants commonly used in conventional air-conditioning systems.

Efficient heat and mass transfer within the absorber and desorber of absorption chillers remains a critical challenge [2]. To address this, various heat exchanger geometries and absorption/desorption processes have been explored to enhance transfer efficiency. Plate heat exchangers (PHEs) with falling films have shown considerable promise, offering high heat and mass transfer coefficients, a compact design, and effective liquid-vapor mixing [3–5]. However, the large size and high initial cost of absorption chillers highlight the need for more compact and cost-effective designs [6]. In such confined heat exchanger geometries, hydrodynamic interactions between the liquid and the vapor at the interface must be carefully considered. These interactions, primarily influenced by the shearing effect of the vapor flow, can affect the liquid film distribution, the film velocity and thickness, the amplitude of the interfacial waves (ripple and disturbance waves), and the appearance of the flooding phenomena. They can also affect the pressure drop and the heat and mass transfer performances [7].

In two-phase flow systems, flooding in a single channel is defined as either the blocking of the channel by the liquid flow [8], or partial to complete reversal of the liquid flow [9]. While turbulent conditions are typically required to induce flooding in unconfined configurations, confined geometries can experience flooding even under laminar conditions. Various studies have investigated flooding, producing extensive experimental data and correlations to predict its onset in rectangular channels [10–13] and packed columns [14]. However, discrepancies between these correlations remain unresolved [10]. Furthermore, no experimental studies on the plate heat exchangers of absorption chillers with confined geometries have been identified in the literature.

Thus, the current work aims to develop an experimental setup to test multiple confinement levels of plate heat exchangers and examine flow hydrodynamics in such confined geometries. The counter-current flow configuration, where the liquid and vapor are in opposite directions, was chosen for this study. This configuration reflects the conditions within the generator of an absorption chiller, where flooding is most likely to occur and must be prevented. Additionally, the study seeks to determine the conditions leading to the onset of flooding in these systems.

2. Experimental setup

The experimental setup was designed to simulate grooved plates similar to those used in the generator studied by Wirtz et al. [15]. Grooved plates were specifically chosen instead of conventional plate heat exchanger geometries to address the wetting issues typically encountered in conventional designs. By introducing channels with controlled dimensions to the plates, the setup aimed to achieve a better wetting behavior. The key difference between the tested plates was the channel height, which was varied at 4 mm, 2 mm, and 1 mm, while the channel width remained constant at 4 mm for all plates. Each plate consisted of 10 channels. A schematic representation of the setup is provided in Figure 1.

Water from a reservoir was conveyed into the upper part of the channels by a volumetric pump through holes drilled in the wall, ensuring uniform distribution across all channels. The water flow rate was controlled by adjusting the pump's rotational speed. Simultaneously, air was injected uniformly into the lower part of the channels through holes drilled in the wall to create a counter-current configuration, replicating the conditions in the generator. The airflow rate was regulated using an inflow valve. The setup incorporated two flowmeters to measure the flow rates of water and air, along with a differential pressure gauge to monitor the pressure drop across a reference channel, as illustrated in Figure 1. All experiments were conducted under atmospheric conditions, with the operating range and measurement uncertainties detailed in Table 1.

To develop flow pattern map for each plate and identify the conditions leading to flooding phenomena, the total water flow rate was varied from 0 to 20 kg/h, while the airflow rate was adjusted between 0 and 5 L/min. These ranges were selected based on the operational limits of the flowmeters used in the setup.

Table 1: Operating range and uncertainties of the measurements.

Instrument	**Measurement**	**Range**	**Uncertainty**
Water flowmeter	Water flow rate [kg.h^{-1}]	0 - 20	±0.7%
Air flowmeter	Air flow rate [L.min^{-1}]	0 - 5	±1.46%
Differential pressure gauge	Pressure drop [mbar]	0-10	±0.038 mbar

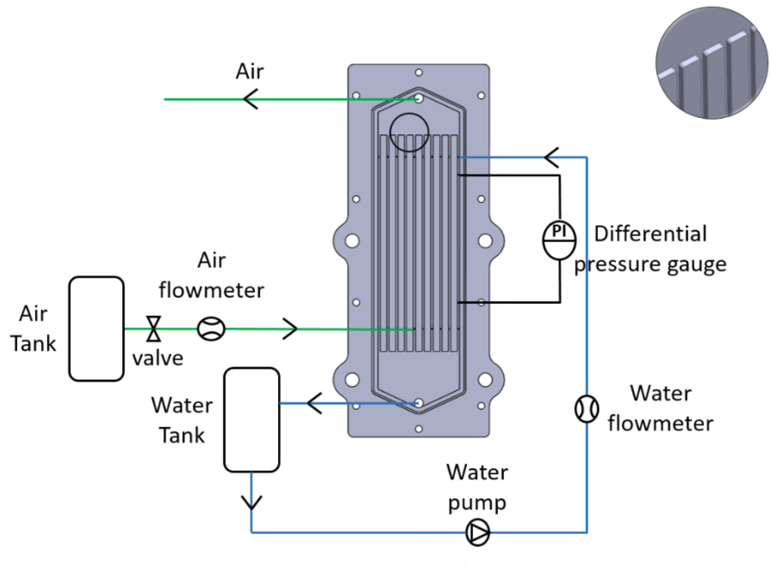

Figure 1: Schematic representation of the experimental setup.

3. Results & Analysis

For each plate configuration, the water distribution within the channels was analysed, and the flow rates of both water and air associated with the appearance of the flooding phenomena were identified.

3.1. Flooding phenomena

The extensive experimental data obtained has enabled the identification of different types of flooding, as illustrated in Figure 2. These flooding types align with the classification defined by researchers, as described in Section 1. The first type of flooding is characterized by the formation of a water plug that obstructs the airflow. The second type involves a partial reversal of the liquid film, while the third and final type is marked by a complete reversal of the liquid film, causing the flow direction to shift from downward to upward.

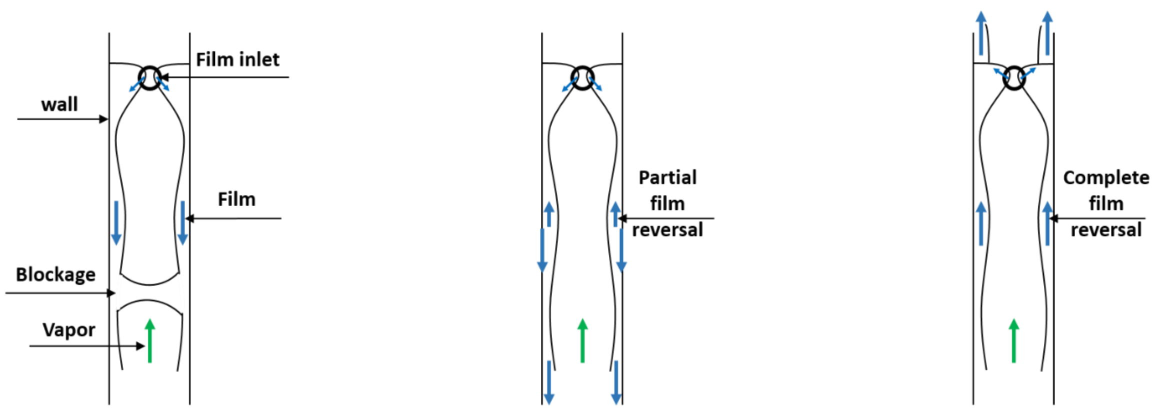

a) Type 1 *b) Type 2* *c) Type 3*

Figure 2: Flooding types.

To gain a deeper understanding of the first type of flooding, as well as the formation and stability of the water plug, a force balance is performed. This will clarify the influence of the various forces on the plug's stability. Let us consider a liquid plug of height (*H*) in equilibrium within a vertical rectangular channel of height (*e*) and width (*W*) as illustrated in Figure 3. Properties related to the upper meniscus and the region above the plug are marked with subscript 1, while those related to the lower region are marked with subscript 2. The forces acting on the liquid volume include:

- The weight $\vec{P} = -m.g.\vec{z}$,
- The resultant pressure force F_p,
- Capillary forces: acting at the contact lines, represented by vectors F_1 and F_2.

By neglecting curvature effects of the menisci for the calculation of the volume of the plug, the force balance along the z-axis leads to the following equation:

$$-\rho_L.g.W.e.H + (P_2 - P_1).W.e + 2.\sigma.(\cos\theta_1 - \cos\theta_2).(W + e) = 0 \qquad (1)$$

The balance between the three resultant forces ensures the stability of the water plug in the channel.

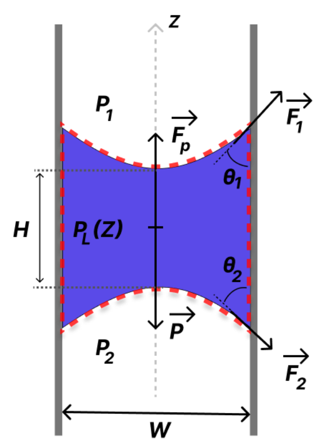

Figure 3 : Equilibrium of a liquid plug in a rectangular channel.

3.2. Flow distribution & flooding appearance across the studied channel heights

The pressure drop across a reference channel was measured using a differential pressure gauge. The pressure drop served as an additional indicator for confirming the occurrence of flooding, complementing the visual observations. Figure 4 illustrates the variation of pressure drop as a function of airflow rate and time for a fixed water flow rate of 14 kg/h, presented for the two channel heights: 4 mm and 2 mm.

For the 4 mm channel height, the pressure drop increases quasi linearly with the increase of the flow rate. No flooding was observed across all the tested airflow rates. However, for the 2 mm channel height, a sudden increase in pressure drop was observed starting at an airflow rate of 3 L/min, indicating the onset of flooding. This was consistent with visual observations, which identified the flooding as Type 1, characterized by the formation of a water plug in the reference channel, causing the pressure drop to reach significantly high values. For the 1 mm channel height, at a water flow rate of 14 kg/h, the channels were completely filled with water, preventing any measurements from being recorded.

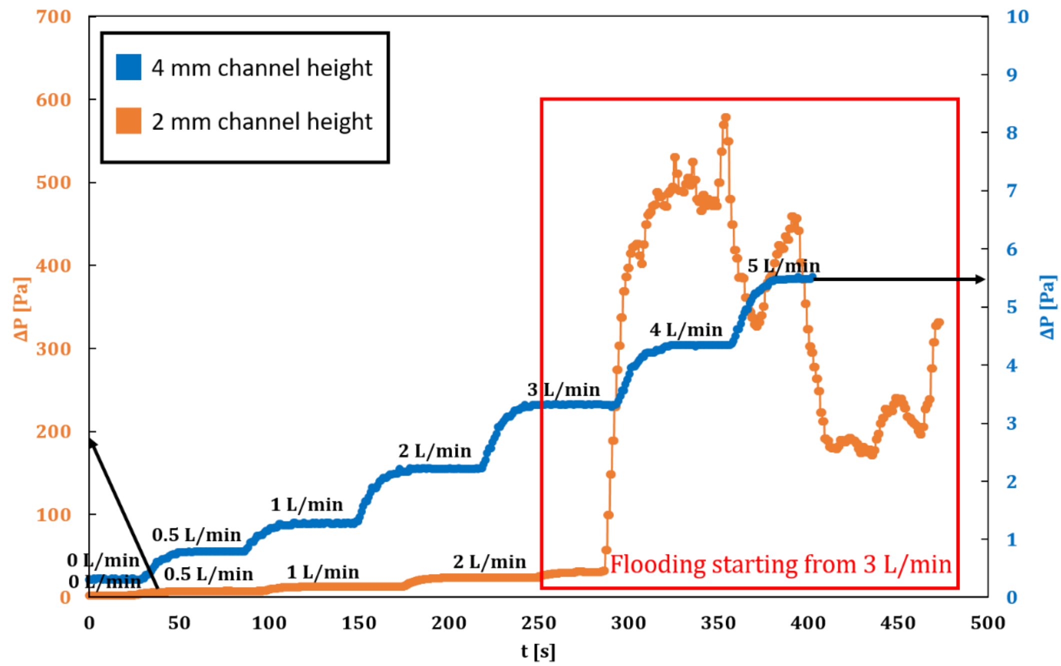

Figure 4: Variation of the pressure drop as a function of the airflow rates and time for a fixed water flow rate of 14 kg/h in 4 mm and 2 mm channel heights.

In addition to detecting the flooding phenomena, the flow distribution within the channels for the different cases was analysed. For the 4 mm channel height, water consistently accumulated in one corner of the rectangular channel across all cases. For the 1 mm channel height, the water was confined to one narrow side of the rectangular channel. However, for the 2 mm channel height, the water distribution varied, appearing on one or both narrow sides of the rectangular channel. Figure 5 shows a high-speed camera image of the 2 mm channel height plate. Three distinct flow configurations are observed: a channel with one wetted narrow wall, a channel with two wetted narrow walls, and a channel exhibiting a water plug. These configurations highlight the varying wetting behaviors and flow patterns within the channels under given experimental conditions.

Figure 6 illustrates the flow distribution within the channels for water flow rates ranging from 5 to 20 kg/h and airflow rates from 0 to 5 L/min. It also highlights the flow conditions under which flooding was detected for the 2 mm channel case in both increasing and decreasing water flow rates, enabling the study of hysteresis phenomena.

For water flow rates between 5 and 11 kg/h, no flooding was observed in any of the tests, regardless of whether the flow rate was increasing or decreasing. However, the hysteresis phenomenon was evident within this range when transitioning from increasing to decreasing water flow rates in terms of flow distribution. Specifically, when increasing the water flowrate from 5 to 11 kg/h, the water predominantly occupies one side of the channel for nearly all channels on the plate. In contrast, when decreasing the water flowrate from 11 to 5 kg/h, the water distributes across two sides of the channel in most cases. This behavior is primarily attributed to the initial wetting state of the channel, which serves as the main cause of the hysteresis phenomenon.

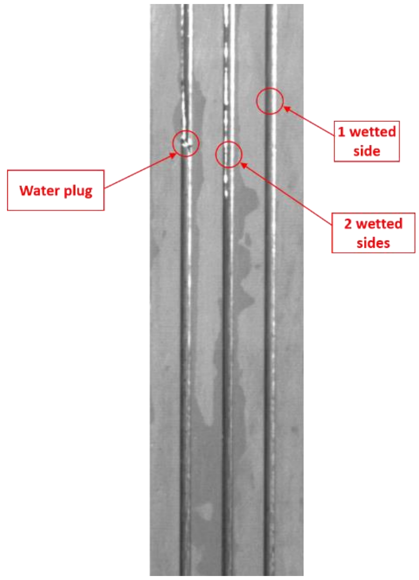

Figure 5 : Flow configurations captured by High-speed camera for a 2 mm channel height plate

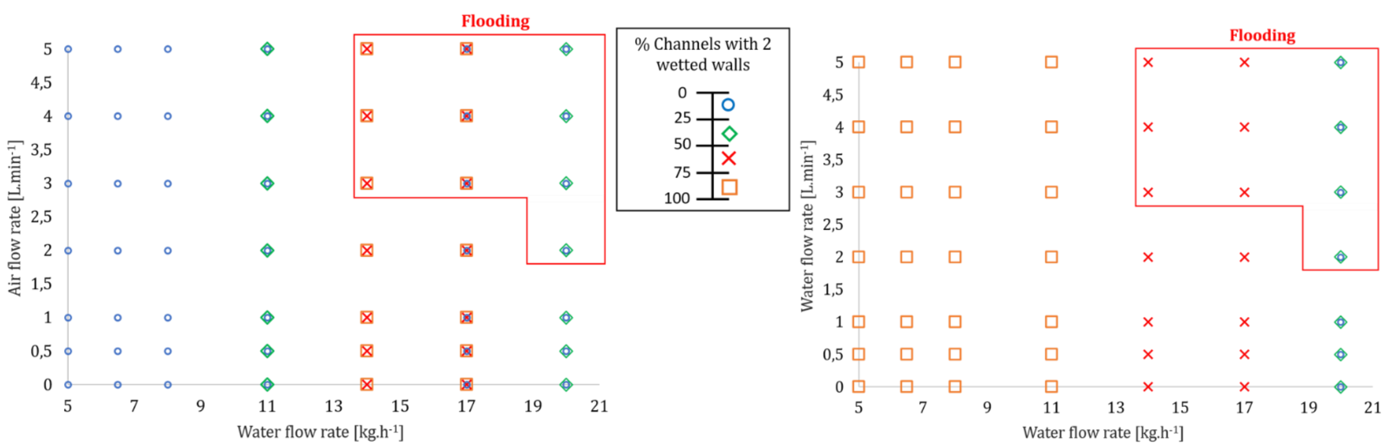

a) Increasing order *b) Decreasing order*

Figure 6: Flow distribution and flooding in 2 mm height channel under increasing and decreasing water flow rates from 5 to 20 kg/h.

4. Conclusion

In this study, an experimental setup was developed to simulate different levels of confinement in falling film plate heat exchangers used in absorption chillers. The primary objective was to investigate the onset of flooding and the flow distribution within the heat exchanger plates, as flooding is a critical phenomenon that must be avoided to ensure the efficiency and reliability of absorption chillers. Three plate geometries were tested, ranging from standard configurations to more confined designs. The results presented in this paper highlight the influence of confinement on flow distribution and the conditions leading to the onset of flooding in such systems. They also suggest that the 2mm channel height geometry appears promising for achieving greater compactness. However, it is essential to consider the flooding limit under operating conditions. Thus, this work provides valuable insights into the operational limits of plate heat exchangers under varying confinement, offering guidance for their design and optimization in practical applications.

Acknowledgements
The authors would like to thanks the Commissariat à l'Energie Atomique et aux Energies Alternatives (CEA) for supporting this work.

References

[1] 'Sustainable, Affordable Cooling Can Save Tens of Thousands of Lives Each Year', *IEA*, Mar. 2023.

[2] C. Zhai and W. Wu, 'Performance optimization and comparison towards compact and efficient absorption refrigeration system with conventional and emerging absorbers/desorbers', *Energy*, vol. 229, p. 120669, Aug. 2021. DOI: 10.1016/j.energy.2021.120669.

[3] Y. T. Kang, A. Akisawa, and T. Kashiwagi, 'Analytical investigation of two different absorption modes: falling film and bubble types', *Int. J. Refrig.*, 2000. .

[4] F. Táboas, M. Vallès, M. Bourouis, and A. Coronas, 'Assessment of boiling heat transfer and pressure drop correlations of ammonia/water mixture in a plate heat exchanger', *Int. J. Refrig.*, vol. 35, no. 3, pp. 633–644, May 2012. DOI: 10.1016/j.ijrefrig.2011.10.003.

[5] D. Triché, S. Bonnot, M. Perier-Muzet, F. Boudéhenn, H. Demasles, and N. Caney, 'Experimental and numerical study of a falling film absorber in an ammonia-water absorption chiller', *Int. J. Heat Mass Transf.*, vol. 111, pp. 374–385, Aug. 2017. DOI: 10.1016/j.ijheatmasstransfer.2017.04.008.

[6] A. M. Abed, M. A. Alghoul, K. Sopian, H. Sh. Majdi, A. N. Al-Shamani, and A. F. Muftah, 'Enhancement aspects of single stage absorption cooling cycle: A detailed review', *Renew. Sustain. Energy Rev.*, vol. 77, pp. 1010–1045, Sep. 2017. DOI: 10.1016/j.rser.2016.11.231.

[7] C.-Y. Zhao, L.-W. Liang, D. Qi, W.-T. Ji, and W.-Q. Tao, 'The effect of gas streams on the hydrodynamics, heat and mass transfer in falling film evaporation, absorption, cooling and dehumidification: A comprehensive review', *Build. Environ.*, vol. 219, p. 109183, Jul. 2022. DOI: 10.1016/j.buildenv.2022.109183.

[8] N. A. Vlachos, S. V. Paras, A. A. Mouza, and A. J. Karabelas, 'Visual observations of flooding in narrow rectangular channels', *Int. J. Multiph. Flow*, vol. 27, no. 8, pp. 1415–1430, Aug. 2001. DOI: 10.1016/S0301-9322(01)00009-X.

[9] S. Jayanti, A. Tokarz, and G. F. Hewitt, 'Theoretical investigation of the diameter effect on flooding in countercurrent flow', *Int. J. Multiph. Flow*, vol. 22, no. 2, pp. 307–324, Apr. 1996. DOI: 10.1016/0301-9322(95)00069-0.

[10] A. Biton, E. Rabinovich, and E. Gilad, 'Generalized correlation for onset flooding velocity in vertical channels', *Int. Commun. Heat Mass Transf.*, vol. 138, p. 106366, Nov. 2022. DOI: 10.1016/j.icheatmasstransfer.2022.106366.

[11] M. Osakabe and Y. Kawasaki, 'Top flooding in thin rectangular and annular passages', *Int. J. Multiph. Flow*, vol. 15, no. 5, pp. 747–754, Sep. 1989. DOI: 10.1016/0301-9322(89)90038-4.

[12] Y. Sudo, T. Usui, and M. Kaminaga, 'Experimental Study of Falling Water Limitation under a Counter-Current Flow in a Vertical Rectangular Channel : 1st Report, Effect of Flow Channel Configuration and Introduction of CCFL Correlation', *JSME Int. J. Ser 2 Fluids Eng. Heat Transf. Power Combust. Thermophys. Prop.*, vol. 34, no. 2, pp. 169–174, 1991. DOI: 10.1299/jsmeb1988.34.2_169.

[13] E. I. P. Drosos, S. V. Paras, and A. J. Karabelas, 'Counter-current gas–liquid flow in a vertical narrow channel—Liquid film characteristics and flooding phenomena', *Int. J. Multiph. Flow*, vol. 32, no. 1, pp. 51–81, Jan. 2006. DOI: 10.1016/j.ijmultiphaseflow.2005.07.005.

[14] A. Pieck, C. Crampon, A. Fabien, and E. Badens, 'A new correlation for predicting flooding point in supercritical fractionation packed columns', *J. Supercrit. Fluids*, vol. 179, p. 105404, Jan. 2022. DOI: 10.1016/j.supflu.2021.105404.

[15] M. Wirtz, B. Stutz, H. T. Phan, and F. Boudehenn, 'Combined generator for an NH3–H2O absorption chiller', *Int. J. Heat Mass Transf.*, vol. 196, p. 123311, Nov. 2022. DOI: 10.1016/j.ijheatmasstransfer.2022.123311.